

Bistatic Forward-Looking SAR Imaging Based on Two-Dimensional Principle of Stationary Phase

Jing Li, Shunsheng Zhang, Junfei Chang
Research Institute of Electronic Science and Technology
University of Electronic Science and Technology of China
Chengdu 611731, China
Email: lijing8609@hotmail.com; zhangss@uestc.edu.cn

Abstract—Synthetic aperture radar (SAR) techniques are typically used to achieve a high azimuth resolution, but conventional monostatic SAR is not applicable in forward direction because of azimuth ambiguities and poor Doppler resolution. In this paper, we present a new bistatic forward-looking SAR imaging algorithm based on point target reference spectrum using the two-dimensional(2-D) principle of stationary phase to improve the Doppler resolution and to avoid azimuth ambiguities. Based on the bistatic configuration and the novel algorithm, SAR not only can image the forward-looking terrain of the aircraft, but also plays sufficient role in selflanding and navigation. Finally, simulations are used to validate the proposed spectrum and processing algorithm.

Index Terms — Bistatic ,forward-looking, SAR , principle of stationary phase.

I. INTRODUCTION

Synthetic aperture radar (SAR) is a radar imaging technology that is capable of producing high resolution images of the stationary surface targets. The main advantages of SAR are that it can reduce the effects of clouds and fog and allow them to be independent of external sources for imaging, having day and night and all-weather imaging capability. Conventional monostatic SAR is not applicable in forward direction because of azimuth ambiguities and poor Doppler resolution. To improve the Doppler resolution and to avoid azimuth ambiguities, bistatic SAR configurations can be used to obtain high-resolution radar images. Bistatic SAR uses a separated transmitter and receiver moving on different platforms. This configuration is becoming prospective in the field of Earth remote sensing and mapping due to its attractive features\platform flexibility, immunity to physical attacks and electronic countermeasures [1].

For the bistatic case, the range history is the sum of two hyperbolic range equation, known as the double-square-root term. Therefore, the bistatic point-target reference spectrum does not offer the analytical simplicity of the single square root in monostatic SAR using the principle of stationary phase (PSP). Several methods of solving the spectrum have been researched, such as keystone transform[1], series reversion[2], Loffeled's bistatic formula[3] and two-dimensional(2-D) principle of stationary phase[4].

The bistatic forward-looking SAR uses the spatially separated forward-looking receiver and side-looking transmitter. Bistatic forward-looking radar imaging continues to gain in

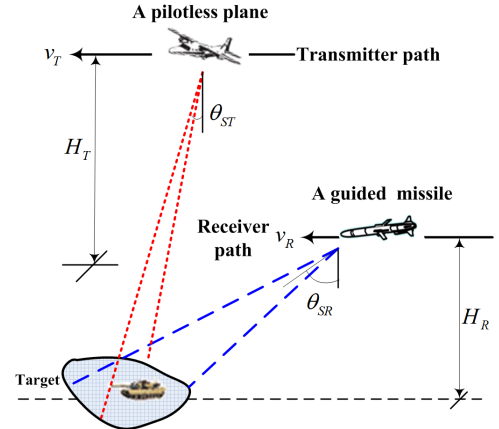


Fig. 1. Geometry of bistatic forward-looking SAR

significance due to a variety of convenient applications, such as flexibility of flight path, reduction of hardware cost, additional information, increased radar cross section and landing assistance for aircraft in poor visibility conditions. Bistatic forward-looking SAR arouses researchers' concern, and a few investigations on bistatic forward-looking SAR have been published. Bistatic forward-looking SAR systems with multiple antennas have been developed [5], several reconstruction methods and experiments are ongoing [6-16].

In this paper, we introduce a novel bistatic forward-looking SAR imaging algorithm based on bistatic configuration and 2-D principle of stationary phase. The key idea in our approach is to use 2-D principle of stationary phase to calculate the spectrum of bistatic forward-looking SAR. This method can accurately calculate the spectrum which contains two hyperbolic range-azimuth coupling terms and thus is very similar to the monostatic spectrum.

The rest of this paper is organized as follows. In Section II, the signal model of bistatic forward-looking SAR is presented. In Section III, the image formation algorithm using 2-D principle of stationary phase is discussed in detail. The results of performance analysis and the experimental results are presented in Section IV. Finally, Section V concludes this paper.

II. SIGNAL MODEL

The geometry configuration of bistatic forward-looking SAR is shown in Fig. 1, where the transmitter and the receiver are mounted on two different platforms. The receiving antenna is forward looking, while the transmitter antenna is squint looking; θ_{SR} is the receivers look-down angle, and θ_{ST} represents the squint angle of the transmitter. The moving velocity of transmitter and receiver are v_T and v_R , respectively. This geometry is of advantage to guide for the missile and has been used in many civilian and military fields with its forward-looking model. $R_R(\eta)$ and $R_T(\eta)$ are the instantaneous slant ranges from the receiver and transmitter to the point target, defined as

$$R_R(\eta) = \sqrt{H_R^2 + (\eta - \eta_{R0})^2 v_R^2} \quad (1)$$

$$R_T(\eta) = \sqrt{R_{T0}^2 + (\eta - \eta_{T0})^2 v_T^2} \quad (2)$$

where η is the slow time. η_{T0} and η_{R0} are the instantaneous slow time of the transmitter and receiver to the sensor position at $\eta = 0$, respectively. R_{T0} is the transmitted range to the sensor position at $\eta = 0$, H_R represents the receiver platform height.

III. IMAGING FORMATION ALGORITHM

Suppose the transmitted signal is linear frequency modulated (LFM) signal. After mixing down and quadrature demodulation, the received radar signal is given by

$$s_R(\eta, t) = \text{rect}\left(\frac{t - R(\eta)/c}{T_p}\right) \times \exp\left\{j\pi k_r \left(t - \frac{R(\eta)}{c}\right)^2 - j\frac{2\pi R(\eta)}{\lambda}\right\} \quad (3)$$

where $R(\eta) = R_T(\eta) + R_R(\eta)$, t is the fast time, T_p is the pulse duration, k_r is the chirp rate and $\text{rect}(\cdot)$ is the stand for the unit rectangular function.

2D-FFT is made toward (3) using 2-D principle of stationary phase[4], then ignore the amplitude, the spectrum expression of bistatic forward-looking echo signal can be described as

$$S(f_\eta, f_t, R_{R0}) = \exp\{-j\Psi(f_\eta, f_t, R_{R0})\} \quad (4)$$

where

$$\Psi(f_\eta, f_t, R_{R0}) = \Phi_{RC}(f_\eta, f_t) + \Phi_{RCM}(f_\eta, f_t, R_{R0}) + \Phi_{AC}(f_\eta, R_{R0}) + \Phi_{AS}(f_\eta) \quad (5)$$

$$\Phi_{RC}(f_\eta, f_t) \approx \pi \frac{f_t}{k_r} - \pi \frac{f_t}{K_{SRC}} \quad (6)$$

$$\Phi_{RCM}(f_\eta, f_t, R_{R0}) = \frac{2\pi}{c} \left[\frac{R_{R0}}{D_R} + \frac{R_{T0}}{D_T} \right] f_t \quad (7)$$

$$\Phi_{AC}(f_\eta, R_{R0}) = 2\pi(p_{10} + p_{11}R_{R0})k_T f_\eta + \frac{2\pi}{\lambda}(R_{R0}D_R + R_{T0}D_T) \quad (8)$$

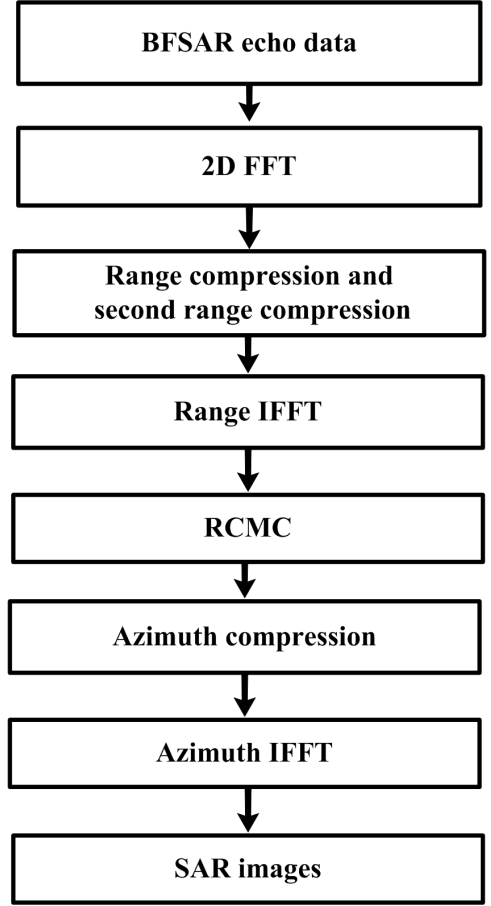


Fig. 2. Block diagram of image formation algorithm for bistatic forward-looking SAR.

$$\Phi_{AS}(f_\eta) = 2\pi\beta_A\eta_{R0}f_\eta \quad (9)$$

and where

$$\frac{1}{K_{SRC}} = R_{R0} \frac{(\mu_{R1} - \mu_{R2})^2}{cf_c D_R^3} + R_{T0} \frac{(\mu_{T1} - \mu_{T2})^2}{cf_c D_T^3} \quad (10)$$

$$\mu_{T1} = \frac{\lambda}{v_T}(k_T f_\eta - \mu_c) \quad \mu_{T2} = -\frac{\lambda}{v_T}\mu_c$$

$$\mu_{R1} = \frac{\lambda}{v_R}(k_R f_\eta + \mu_c) \quad \mu_{R2} = \frac{\lambda}{v_R}\mu_c$$

$$D_R = \sqrt{1 - \mu_{R1}^2} \quad D_T = \sqrt{1 - \mu_{T1}^2}$$

$$\beta_A = k_R + p_{12}k_T$$

$$\eta_{T0} = p_{10} + p_{11}R_{R0} + p_{12}\eta_{R0} \quad (11)$$

Substituting (6)-(11) into (5), we can find that the bistatic forward-looking spectrum. Φ_{RC} , Φ_{RCM} , Φ_{AC} , Φ_{AS} represent the range compression term, range cell migration(RCM) term, azimuth compression term, and azimuth scaling term, respectively. Based on (5), the range-doppler algorithm is shown in Fig.2.

TABLE I
SIMULATED RADAR PARAMETERS

Parameters	Value
Carrier frequency	10GHz
Transmitted signal bandwidth	150MHz
Transmitter height	8km
Receiver height	2km
Transmitter velocity	300m/s
Receiver velocity	200m/s
Pulse duration	10μs
PRF	300Hz
θ_{ST}	0°
θ_{SR}	60°

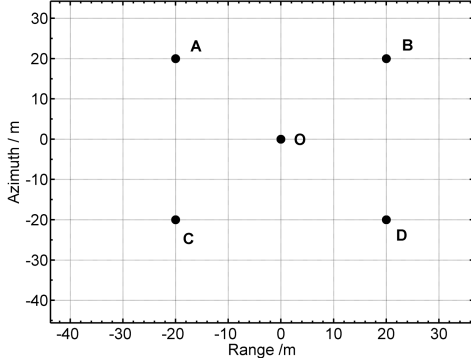


Fig. 3. Simulated scene with five point targets.

IV. SIMULATIONS RESULTS

Simulated data have been used to validate the algorithm in this paper. In following experiments, we set the simulation radar parameters as listed in Table I.

The simulated scene consists of five point targets as shown in Fig.3. Point O is located in the center of the scene, and the other four targets are located on the vertices of a $500m \times 500m$ square. The relative coordinates are listed as follows (m, m) : $O(0, 0)$, $A(20, -20)$, $B(20, 20)$, $D(-20, 20)$, $C(-20, -20)$. Using the parameters of table I, the 5 point targets are reconstructed by the proposed algorithm. The results are shown in Fig.4.

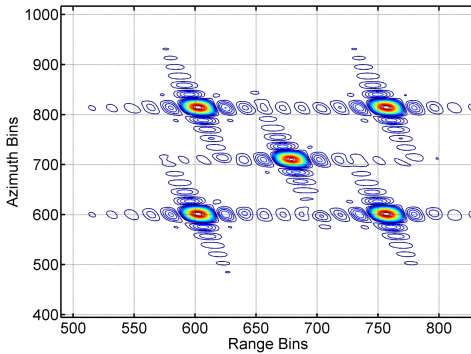


Fig. 4. Contour plots of targets O,A,B,C and D using proposed algorithm.

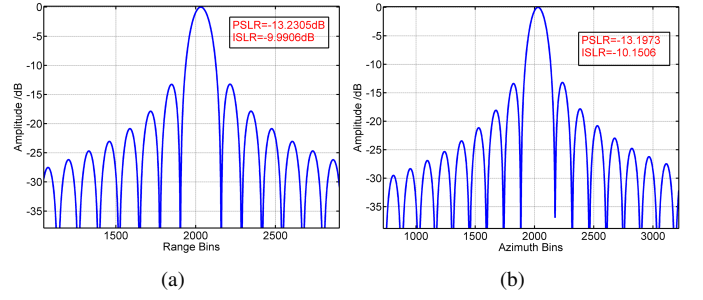


Fig. 5. Range and azimuth compression simulation results. (a) The range profile of target O . (b) The azimuth profile of target O .

TABLE II
POINT-TARGET IMAGING PERFORMANCE

		PSLR(dB)	ISLR(dB)
Point A	Range	-13.2628	-10.0262
	Azimuth	-13.1375	-10.0245
Point B	Range	-13.2758	-10.0288
	Azimuth	-13.2012	-10.1149
Point C	Range	-13.3071	-10.0834
	Azimuth	-13.1583	-10.0974
Point D	Range	-13.2536	-10.0015
	Azimuth	-13.1905	-10.1347

Furthermore, we use the Peak Side-lobe Ratio (PSLR) and the Integrated Side-lobe Ratio (ISLR) as measurement of performance to evaluate the reconstructed point target. The point target O located at the central scene is used for measurement. The results of the range and azimuth profile are shown in Fig.5. The other four point targets imaging performance are shown in Table II. From Fig.5 and Table II, we can find that this proposed method has good imaging performance.

V. CONCLUSION

In this paper, 2-D principle of stationary phase is used in bistatic forward-looking SAR configuration. Based on this method, the spectrum is divided into the range compression term, RCM term, azimuth compression term, and azimuth scaling term, thus is very similar to the monostatic spectrum. In terms of on the spectrum, the bistatic forward-looking Range-Doppler algorithm is proposed. Because of the novel algorithm, SAR not only can image the forward-looking terrain of the aircraft, but also play sufficient role in selflanding, navigation. Finally, the simulation experiments and performance analysis verify the validity of the proposed bistatic forward-looking imaging algorithm.

ACKNOWLEDGMENT

This work was supported by the Fundamental Research Funds for the Central Universities of China under NO.ZYGX2010J118.

REFERENCES

- [1] C.Y. Dai and X.L. Zhang, "Bistatic SAR image formation algorithm using keystone transform", in *Proc IEEE Radar Conf.*, May.2011,pp.342-345.

- [2] Y. L. Neo, F. Wong, and I. Cumming, "A two-dimensional spectrum for bistatic sar processing using series reversion", *IEEE Geosci. Remote Sens. Lett.*, vol. 4, no. 1, pp. 93-96, Jan, 2007.
- [3] O. Loffeld, H. Nies, V. Peters, and S. Knedlik, "Models and useful relations for bistatic sar processing", *IEEE Trans. Geosci. Remote Sens.*, vol. 42, no. 10, pp. 2031-2038, Oct. 2004.
- [4] R. Wang, Y. K. Deng, O. Loffeld, H. Nies, I. Walterscheid, T. Espeter, J. Klare and Joachim H. G. Ende, "Processing the azimuth-variant bistatic SAR data by using monostatic imaging algorithms based on two-dimensional principle of stationary phase", *IEEE Trans. Geosci. Remote Sens.*, vol. 49, no. 10, pp. 3504-3520, Apr. 2011.
- [5] S. Dai, M. Liu, Y. Sun, and W. Wiesbeck, "The latest development of high resolution imaging for forward looking SAR with multiple receiving antennas", in *Proc. IGARSS, Sydney, Australia, 2001*, vol. 3, pp. 1433-1435.
- [6] Hee-Sub Shin and Jong-Tae Lim, "Omega-k algorithm for airborne forward-looking bistatic spotlight SAR imaging", *IEEE Geosci. Remote Sens. Lett.*, vol. 6, no. 2, pp. 312-316, Apr, 2009.
- [7] T. Espeter, I. Walterscheid, J. Klare, A. R. Brenner and Joachim H. G. Ender, "Bistatic Forward-Looking SAR: Results of a spaceborne/airborne experiment", *IEEE Geosci. Remote Sens. Lett.*, vol. 8, no. 4, pp. 765-768, Jul, 2011.
- [8] W. C. Li, Y. L. Huang, J. Y. Yang, J. J. Wu, and L. J. Kong, "An improved radon-transform-based scheme of doppler centroid estimation for bistatic forward-looking SAR", *IEEE Geosci. Remote Sens. Lett.*, vol. 8, no. 2, pp. 379-383, Mar, 2011.
- [9] X. Qiu, D. Hu, and C. Ding, "Some reflections on bistatic SAR of forward-looking configuration", *IEEE Geosci. Remote Sens. Lett.*, vol. 5, no. 4, pp. 735-739, Oct, 2008.
- [10] J. Balke, "Field test of bistatic forward-looking synthetic aperture radar", *IEEE International Radar conference.*, May 2005, Virginia, USA, pp. 424-429.
- [11] I. Walterscheid, T. Espeter, J. Klare, and A. Brenner, "Bistatic spaceborne-airborne forward-looking SAR", *EUSAR 2010.*, Aachen, Germany, Jul, 2010.
- [12] D. Zeng, T. Zeng, C. Hu, and T. Long, "Back-projection algorithm characteristic analysis in forward-looking bistatic SAR", in *Proc. CIE Radar Conf.*, Shanghai, China, Oct. 2006, pp. 1-4.
- [13] C. Hu, T. Zeng, T. Long, and C. Yang, "Forward-looking bistatic SAR range migration algorithm", in *Proc. CIE Radar Conf.*, Shanghai, China, Oct. 2006, pp. 1-4.
- [14] G. Krieger, J. Mittermayer, M. Wendler, F. Witte, and A. Moreira, "SIREV-Sector imaging radar for enhanced vision", in *Proc. Int. Symp. ISPA.*, Jun. 19C21, 2001, pp. 377-382.
- [15] J. Balke, "Bistatic forward-looking synthetic aperture radar", in *Proc. RADAR.*, Toulouse, France, Oct. 2004.
- [16] J. Wu, J. Yang, H. Yang, and Y. Huang, "Optimal geometry configuration of bistatic forward-looking SAR", in *Proc. IEEE Int. Conf. Acoust., Speech, Signal Process.*, 2009, pp. 1117-1120.